

# **Spectro-Spatial Unmixing in Optical Microspectroscopy for Thickness Determination of Layered Materials**

Julian Schwarz,\* Michael Niebauer, Lukas Römling, Adrian Pham, Maria Koleśnik-Gray, Peter Evanschitzky, Nicolas Vogel, Vojislav Krstić, Mathias Rommel, and Andreas Hutzler\*

Van der Waals materials and devices incorporating them exhibit highly thickness-dependent properties. The small lateral dimensions of mechanically exfoliated 2D-layered flakes, however, remarkably complicate their precise thickness determination. Quantitative analysis of reflectance measurements using optical microspectroscopy is proven to be as precise as spectroscopic ellipsometry while providing an easily adaptable and non-destructive method for thickness determination. The use of magnifying objective lenses allows obtaining the reflectance within a measurement spot of only a few microns in diameter. When the dimensions of exfoliated flakes are even smaller, however, the acquired reflectance is a superposition of those of the material of interest and the subjacent materials. To overcome this limitation, a facile approach to reduce the resolvable structure size by combining the evaluation of the reflectance measurement via transfer matrix method with spatial information extracted from optical micrographs is introduced. The efficacy when characterizing micrometer-sized flakes is exemplarily demonstrated for thickness determination of highly oriented pyrolytic graphite and a thin film of silicon dioxide. It is shown that a maximum error of less than 10% is achieved even when the flake only covers 20% of the measurement spot.

1. Introduction

2D-layered so-called van der Waals materials are a promising material class for future (opto-)electronic devices since they exhibit extraordinary optical<sup>[1,2]</sup> and electrical properties.<sup>[3,4]</sup> The full exploitation of these benefits requires a profound knowledge of the exact material thickness, since many electrical and optical parameters depend on the number of layers.[5]

Microspectroscopy has been established as a measurement technique for assessing 2D-layered material thickness in an experimentally simple setup, as depicted in Figure 1a, and thus can be used as an alternative to more demanding characterization methods such as atomic force microscopy (AFM) or Raman microspectroscopy.

The measurement setup merely contains an optical microscope and a spectrometer connected with a glass fiber. Usually, an objective lens focuses a (halogen) light source onto the region of interest and the reflected light is coupled into a spectrometer and a CCD camera. In our previous works, we introduced several approaches for the precise determination of layer thickness via optical microspectroscopy.<sup>[6,7]</sup> However, despite the small spot size in the µm range that can be achieved with microspectroscopy, the size of exfoliated flakes can be smaller and thus prevents accurate measurements.

When fabricating devices, the area accessible for measuring might even be smaller since electrical contacts have to be defined on top, which can mask sections of the flake.[8,9]

In literature, several models exist to account for varying material stacks and/or thicknesses caused by the presence of multilayered parts of a 2D material within a single measurement spot. For

J. Schwarz, M. Niebauer, A. Pham, A. Hutzler Friedrich-Alexander-Universität Erlangen-Nürnberg (FAU) **Electron Devices** Cauerstraße 6, 91058 Erlangen, Germany

E-mail: julian.schwarz@fau.de; andreas.hutzler@fau.de L. Römling, N. Vogel

Friedrich-Alexander-Universität Erlangen-Nürnberg (FAU) Institute of Particle Technology

Cauerstraße 4, 91058 Erlangen, Germany

The ORCID identification number(s) for the author(s) of this article can be found under https://doi.org/10.1002/adom.202402502

© 2024 The Author(s). Advanced Optical Materials published by Wiley-VCH GmbH. This is an open access article under the terms of the Creative Commons Attribution License, which permits use, distribution and reproduction in any medium, provided the original work is properly

DOI: 10.1002/adom.202402502

M. Koleśnik-Gray, V. Krstić Department of Physics Friedrich-Alexander-Universität Erlangen-Nürnberg (FAU) Staudtstraße 7, 91058 Erlangen, Germany

P. Evanschitzky, M. Rommel

Fraunhofer Institute for Integrated Systems and Device Technology IISB Schottkystraße 10, 91058 Erlangen, Germany

Department of Physics Wake Forest University

27109 Winston-Salem NC, United States

A. Hutzler

Forschungszentrum Jülich GmbH

Helmholtz Institute Érlangen-Nürnberg for Renewable Energy (IET-2) Cauerstraße 1, 91058 Erlangen, Germany

//onlinelibrary.wiley.com/terms-and-conditions) on Wiley Online Library for rules of use; OA articles are governed by the applicable Creative Commons License

www.advancedsciencenews.com



www.advopticalmat.de

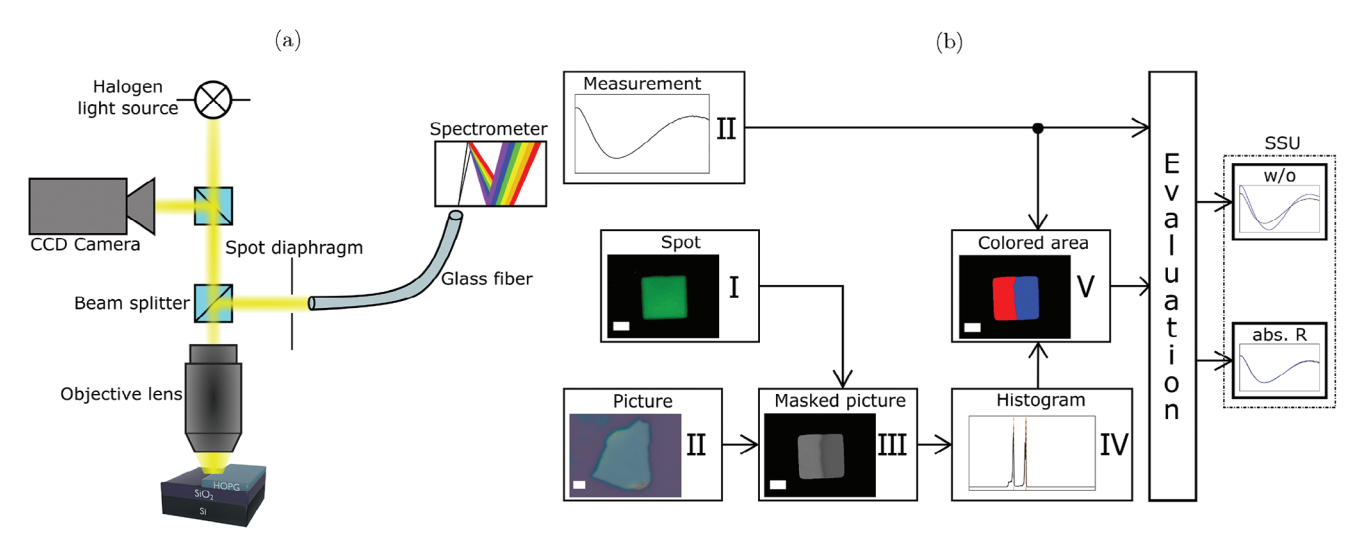


Figure 1. a) Schematic presentation of the measurement setup used for microspectroscopy. b) Flow chart of data processing when using spectro-spatial unmixing (SSU). The scale bars each represent 2 μm.

ellipsometry, a so-called "island-film model" has originally been proposed for the in situ investigation of ellipsometric parameters and the refractive index during the growth process of submonolayer Pb on Ag and Cu substrates. [10] Recently, this "islandfilm model" was revisited for the determination of a dispersion model of mono-layer domains of MoS<sub>2</sub><sup>[11]</sup> and graphene<sup>[12]</sup> or thicker  ${\rm MoS_2}$  and  ${\rm WS_2}$  flakes<sup>[13,14]</sup> surrounded by uncovered regions where the substrate is exposed. Additionally, area weighting was previously established in spectroscopic ellipsometry (SE) for controlling etch processes and step heights.<sup>[15,16]</sup> However, for SE the required lateral dimensions of the material are considerably larger than in the case of microspectroscopy. For reflectometry, an early application was the in situ monitoring of adjacent areas with different etch rates.[17,18] Another instance of area weighting was the phase correction in heterodyne interferometry for surface profiling.<sup>[19]</sup> Several studies also apply such models to through-silicon vias (TSVs), where the lateral dimensions are similar to the ones examined in this work. [20,21] Though, for TSVs the vertical dimensions are much larger, which has a tremendous influence on the measured spectra due to more pronounced interference effects. While the methodology considered in this work is comparable to the "island-film model," the requirements for microspectroscopy, especially the combination of lateral and vertical dimensions, are different and have not been discussed in detail before.

Herein, we present a novel approach to reduce the resolvable structure size of optical microspectroscopy to determine the thickness of 2D material flakes smaller than the actual measurement spot. Therefore, we extract the spectral information of the material of interest from the superimposed reflectance spectrum by exploiting the area fraction distribution in the measurement spot, in the following denoted as spectro-spatial unmixing (SSU).

One advantage of microspectroscopic measurements is that in addition to the spectral information, a microscopic image of the specimen can be acquired, which can be subject to image analysis as well. For instance, if the contrast is sufficient, information about the area coverage of each material and/or different

thicknesses of materials present in the measurement spot can be deduced from the RGB channels of the image. The apparent color of the material stacks emerges from the interference and diffraction effects of the incoming and reflected light waves. In this work, we use this areal information to examine 2D materials that do not completely cover the measurement spot. This is feasible if a sufficiently large, homogeneous area (which has to be large enough to cover the entire measurement spot) of the subjacent or surrounding material (stack) is available.

The basic principle of our approach is shown in Figure 1b. The individual steps to implement this spectro-spatial unmixing (SSU) approach are shortly explained in the following (for more detailed information see the Experimental Section and the Supporting Information). First, we acquire a micrograph of the measurement spot projected onto the image plane (in this work a quadratic spot with a minimum edge length of 5 µm) by illuminating a homogeneous sample or substrate via the glass fiber coupled to an LED from the spectrometer side (Figure 1b-I). Afterward, the sample's reflectance spectrum is recorded and a microscope image is captured alongside (Figure 1b- II). The picture of the measurement spot is then used on the micrograph of the sample to mask the area where the reflectance spectrum was acquired. The masked picture is converted into a gray scale image and its histogram is evaluated (Figure 1b-III,IV). Based on the histogram, the area fraction of the material of interest within the measurement spot is calculated (Figure 1b-V). Under the presumption that the measured reflectance is a "coherent superposition"[10] of individual reflections from the different material stacks within the measurement spot, the spectra of these stacks are weighted according to their calculated area fractions and combined into a model for the effective reflectance in the spot. Finally, the thickness of the investigated material can be determined by comparing the measured superimposed reflectance and the modeled effective reflectance. For precise reflectance modeling of even anisotropic materials, a 4 × 4 transfer matrix method (TMM) as well as corrections for the numerical aperture (NA) of the objective lens are used, as described elsewhere.[7]

21951071, 2025, 5, Downloaded from https://advanced.onlinelibrary.wiley.com/doi/10.1002/adom.202402502 by Forschungszentrum Jülich GmbH Research Center, Wiley Online Library on [21/02/2025]. See the Terms and Conditions (https://advanced.onlinelibrary.wiley.com/doi/10.1002/adom.202402502 by Forschungszentrum Jülich GmbH Research Center, Wiley Online Library on [21/02/2025]. See the Terms and Conditions (https://advanced.onlinelibrary.wiley.com/doi/10.1002/adom.202402502 by Forschungszentrum Jülich GmbH Research Center, Wiley Online Library on [21/02/2025]. See the Terms and Conditions (https://advanced.onlinelibrary.wiley.com/doi/10.1002/adom.202402502 by Forschungszentrum Jülich GmbH Research Center, Wiley Online Library on [21/02/2025]. See the Terms and Conditions (https://advanced.onlinelibrary.wiley.com/doi/10.1002/adom.202402502 by Forschungszentrum Jülich GmbH Research Center, Wiley Online Library on [21/02/2025]. See the Terms and Conditions (https://advanced.onlinelibrary.wiley.com/doi/10.1002/adom.202402502 by Forschungszentrum Jülich GmbH Research Center, Wiley Online Library on [21/02/2025]. See the Terms and Conditions (https://advanced.onlinelibrary.wiley.com/doi/10.1002/adom.202402502 by Forschungszentrum Jülich GmbH Research Center, Wiley Online Library on [21/02/2025]. See the Terms and Conditions (https://advanced.onlinelibrary.wiley.com/doi/10.1002/adom.202402502 by Forschungszentrum Jülich GmbH Research Center (https://advanced.onlinelibrary.wiley.com/doi/10.1002/advanced.onlinelibrary.wiley.com/doi/10.1002/advanced.onlinelibrar

conditions) on Wiley Online Library for rules of use; OA articles are governed by the applicable Creative Commons License

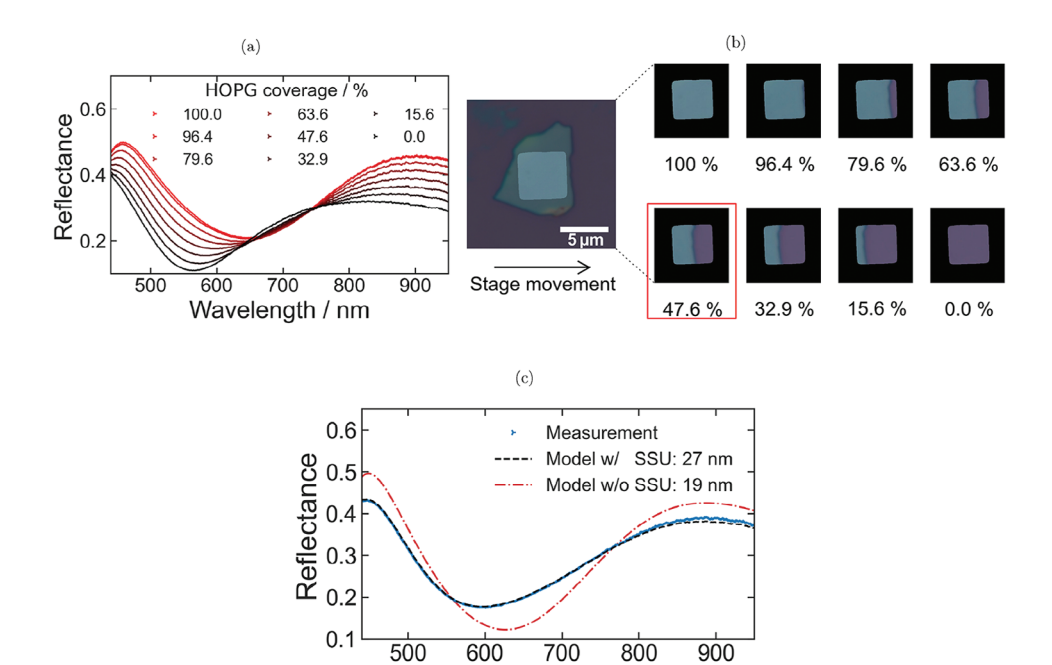


Figure 2. Measured reflectance spectra of HOPG sample 1 for different values of area coverage. b) Overview of the measurement series for accomplishing different values of area coverage of the measurement spot by the same HOPG sample. On the left, an image of the sample is presented with an overlay of the measurement spot of  $5 \, \mu m \times 5 \, \mu m$ . On the right, the masked measurement spot for a continuous stage movement transverse to a sample edge is shown. In addition, the corresponding area percentage of HOPG within the measured area is written below. c) Exemplary comparison of measurement and modeling with and without SSU for a HOPG sample 1 for an area coverage of 47.6%. The corresponding microscope image is depicted with a red frame in Figure 2b.

Wavelength / nm

When employing spectroscopic means, the thickness of isotropic thin films or 2D-layered materials is usually evaluated via analyzing either the absolute reflectance or the contrast (i.e. the differential reflectance referring to the substrate). [22–25] While doing so, either the entire spectrum or the position of extreme values [6,26] can be utilized. The SSU approach proposed in this work is based on modeling the full spectrum of a measured absolute reflectance (denoted as *abs. R* in Figure 1b). Here, the measurement spot covers two different regions, where one region consists of the whole stack including the material of interest on top of an underlying material stack and the other region consists of the underlying material stack only (from here on simply referred to as substrate).

In the following, the capability of the proposed SSU approach is demonstrated for two exemplary material combinations in the measurement spot: a thin film of  $SiO_2$  on a Si substrate and highly oriented pyrolytic graphite (HOPG) on a Si substrate coated with  $SiO_2$ .

## 2. Results and Discussion

Subsequently, the area fraction of the measurement spot covered by the material of interest is denoted as the coverage by the material of interest. To characterize the effectiveness of our approach, we tested different values of area coverage for exemplary thin films within the measurement spot. In **Figure 2**a the reflectance of a HOPG sample on 300 nm  $\text{SiO}_2/\text{Si}$  substrate (HOPG sample 1) is depicted for varying coverage by HOPG. Here, the mea-

surement result for a coverage of 0% corresponds to the pure substrate spectrum, i.e. SiO<sub>2</sub> on Si. A gradual change in the spectrum is visible with increasing coverage. Figure 2b exemplarily illustrates the procedure for measuring the reflectance of varying area coverage by HOPG with a quadratic measurement spot with 5 µm edge length. On the left side, an enlarged section of the camera image is depicted containing the entire sample. In addition, the corresponding measurement spot completely covered by HOPG (area fraction of 100%) is shown as an overlay for orientation. Within a measurement series, the microscope stage was moved sequentially in small steps and transversely to a sample edge to obtain varying values of area coverage by the different material stacks within the measurement spot. On the right side the masked images corresponding to the individual measurements are presented and, in addition, the area fractions obtained are attached. For the case as shown in the micrograph with a HOPG coverage of 47.6% (indicated by a red frame), the measured reflectance is exemplarily depicted in Figure 2c together with the modeled reflectance including SSU as well as the modeled reflectance without considering SSU as a baseline. While in the case of the SSU the spatial information about the coverage within the measurement spot is exploited, the modeling without SSU assumes a homogeneous thin film filling the whole measured area and consequently results in a large error in modeling the reflectance. Precise agreement with the measurement is accomplished for the model with SSU whereas the model without SSU shows obvious deviations from the experimental data. This is also reflected in the determined thickness. We first determined

2195 1071, 2025, 5, Downl

oaded from https://advanced.onlinelibrary.wiley.com/doi/10.1002/adom.202402502 by Forschungszentrum Jülich GmbH Research Center, Wiley Online Library on [21/02/2025]. See the Terms and Conditions (https://advanced.online

and-conditions) on Wiley Online Library for rules of use; OA articles are governed by the applicable Creative Commons License

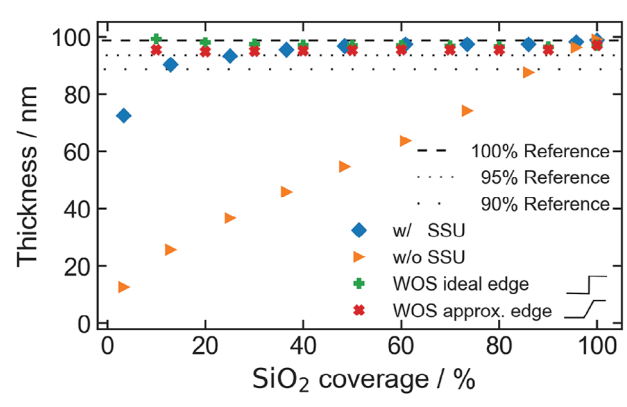


**Figure 3.** Evaluated thicknesses via SSU approach for a  $SiO_2$  film on Si in the edge region to the Si substrate. The values of the reference thickness measured via LE as well as 95% and 90% of this value are marked as dashed/dotted lines. Also shown is the SSU evaluation of spectra simulated using wave optics simulations (WOS) for an idealized and an approximated edge shape.

the absolute film thickness via AFM as 27.7±0.3 nm (mean value and standard deviation). We then compared the result via microspectroscopy of the measurement spot incompletely-covered with HOPG. The thickness determined by analyzing the absolute reflectance exhibits only a small error of ca. 2% with 27.1 nm when using the SSU; without SSU a large error with 18.9 nm is obtained, corresponding to a large relative deviation of around 32%. These results demonstrate the basic applicability of the proposed approach.

**Figure 3** shows the results of the different evaluation approaches for several values of area coverage by a  $SiO_2$  film on a Si substrate. The  $SiO_2$  thickness was measured via laser ellipsometry (LE) for reference and is  $98.5\pm0.3$  nm. The necessary edge to create the desired inhomogeneous coverage to investigate our spectroscopic approach, was prepared via wet chemical etching of one part of the  $SiO_2$  film down to the silicon with HF.

Remarkably, without SSU the modeled thickness significantly deviates from the reference thickness obtained via LE, except for area percentages larger than 90% (orange triangles). For values below 90% the thickness is consequently underestimated, correlating with the area of the  $\mathrm{SiO}_2$  getting smaller. With SSU (blue diamonds), even for smaller area percentages the thickness is close to the reference measurement: The thickness deviates by less than 10% for areas covered with only 12.9% of the targeted  $\mathrm{SiO}_2$  layer. The decreasing thickness for the modeling without SSU is ascribed to the decreasing coverage by  $\mathrm{SiO}_2$ , which is not considered in this case. Therefore, the measured spectrum becomes less similar to a pure  $\mathrm{SiO}_2$  spectrum for low coverage, which results in smaller modeled thicknesses.

Wave optics simulations (WOS) based on Dr.LiTHO, <sup>[27]</sup> a development and research simulator for optical lithography based on rigorous coupled-wave analysis (RCWA), were performed emulating the measurement and sample configuration for different coverage by SiO<sub>2</sub>. <sup>[27]</sup> Besides an idealized edge shape, an edge morphology replicating blurring introduced by the diffraction limited optics was tested. Exemplary reflectance results within the simulated mask replicating the measurement spot for the different edge morphologies are depicted in Figures S1a and S2b

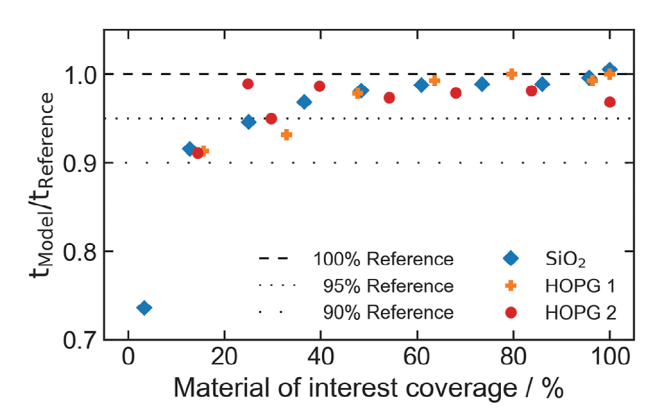


**Figure 4.** Comparison of the thicknesses evaluated from the modeling using the SSU approach based on absolute reflectance values for different samples (an  $SiO_2$  plateau as well as flakes of HOPG). Thickness values are given as relative values normalized to the reference thicknesses (mean values) obtained from LE (98.5 nm for  $SiO_2$ ) or AFM (27.7 nm and 38.3 nm for HOPG) - 95% and 90% of these values are marked as dashed/dotted lines.

(Supporting Information) and an exemplary average reflectance within the simulated mask for the implemented edge morphologies is shown in Figure S1c (Supporting Information). The resulting reflectance spectra (average reflectance calculated for different wavelengths) were analyzed in a similar manner to the measured data within the proposed SSU and TMM approach (the simulated reflectance spectra for different area fractions are shown in Figure S2, Supporting Information). The findings for the wave optics simulations are depicted in Figure 3 as well. For both edge morphologies the determined thickness agrees well with the reference thickness with an error smaller than 5% even for area percentages lower than 20%. Therefore, it can be concluded that the assumption of linear superposition of the reflectance spectra of the individual material stacks is valid. The small deviation is likely from more pronounced diffuse reflection at the edge, which the RCWA simulation takes into account in contrast to the SSU modeling, which only considers the specular component. For a detailed description of the procedure of simulating the reflectance spectra based on wave optics and the analysis thereof see the Supporting Information.

Next, we increase the complexity and use two composite samples each containing a flake of HOPG on a Si wafer with a thermally grown SiO<sub>2</sub> layer with a thickness of 300 nm on top. In Figure 4, we compare the modeling results using SSU for the previously mentioned SiO<sub>2</sub> sample and the HOPG samples with different thicknesses. For better comparability, the modeled thicknesses  $(t_{\text{Model}})$  for the respective area percentages are normalized to the corresponding reference thickness (t<sub>Reference</sub>) obtained via LE for SiO<sub>2</sub> and AFM for HOPG. The AFM results are 27.7±0.3 nm for HOPG sample 1 and 38.3±2.4 nm for HOPG sample 2. The corresponding measured reflectance spectra for the investigated samples with different values of area coverage can be found in Figure S3 (Supporting Information). Since the thickness determination is based on a least square fitting algorithm via a TMM, no metric of uncertainty is deducible from the numerical process. However, the spectral resolution of the spectrometer, i.e., the bandwidth of the spectrometer channels

www.advancedsciencenews.com



www.advopticalmat.de

(i.e., 0.8 nm, according to the actual measurement output) can be considered. Three times the channel bandwidth was used as a safety margin and the measured spectra were shifted by  $\pm 2.4$  nm and the thickness was reevaluated from the shifted spectra.<sup>[7]</sup> The uncertainty determined regarding the thickness is negligible and is presented accompanied by the least square fitting error in Figure S4 (Supporting Information) for reasons of clarity.

Even for the more complex case of HOPG flakes, as an exemplary van der Waals material, our SSU approach can accurately determine the film thickness within an error margin of 5% when the film covers more than 40% of the measurement spot. Overall, we see a continuous decrease in the modeled film thickness, even with the SSU approach, which apparently reaches its limits of applicability here. While the method has basically no numerical limit, we now discuss possible causes for this effect in order to examine the practical boundaries of the model.

In general, the reflectance contribution from the material of interest is diminishing with lower coverage while the other signal parts (including noise and the reflectance of the underlying films) are constant or increase. Thus, the ratio of the reflectance signal collected in the region of interest becomes smaller compared to the noise level and reflectance signal of the substrate and the modeling is therefore less precise. Furthermore, the apparent transition area due to the edge between the material stack of interest and the surrounding material is a source of uncertainty and becomes more significant (larger relative contribution to the area fraction of the material stack of interest) for smaller area percentages of the film of interest (in our example, the HOPG flake). The reason for this is that the relative contribution of the transition area to the total reflectance from areas containing HOPG increases. For the investigated samples, the transition area has a gray value closer to the ambient material stack (i.e., the substrates Si for SiO<sub>2</sub> and SiO<sub>2</sub>/Si for HOPG, for an example see the edge region in Figure 2b) and hence is attributed to this material region for the calculation of the area percentages from the histogram. But in reality, the transition region around the edge exhibits a different reflectance characteristic depending on its shape and dimensions. These properties are not accessible or distinguishable by microspectroscopy or microscope images (pixel size in the image plane below 100 nm) and cannot be clearly resolved because of the limiting optical resolution of the objective lens (Abbe diffraction limit of 333 nm at a wavelength of 500 nm for the employed 100x/NA 0.75 lens<sup>[28]</sup>). Additionally, for very small area fractions (i.e. flake dimensions in the range of the optical resolution), the resolution of the optics plays a role, as the individual material stacks can no longer be clearly resolved in the spectrum and in the micrograph. Furthermore, even the regions adjacent to the edge may exhibit an altered reflectance since the spatial arrangement cannot accurately be reproduced by the 1D model the TMM approach is relying on. One solution could be the transition from a ray optics to a wave optics-based method. However, using finite element methods to solve the equations for wave optics would require an exponentially increased computational effort. Another possible source of inaccuracy is collected light originating from scattering processes at the edge outside the measurement spot, because for wide-field microscopy the illuminated area is larger than the measurement spot. A confocal setup could eliminate such artifacts, e.g., by only illuminating the measurement spot. However, a confocal setup is far more complex in terms of spot alignment than a wide-field setup such as the one used in this study. $^{[29]}$ 

Other sources of uncertainty are many factors influencing the determination of the area fractions. Precise agreement of the focal planes of the camera and the spectrometer is necessary. In addition to the alignment of the focus, there must also be a lateral match, i.e. the real position of the measurement spot must exactly match the position in the camera image. If this is not the case, the area fractions determined do not correspond to those of the reflectance measurement. For a well configured microscope setup the mentioned requirements should always be fulfilled. However, we work at the mechanical (and optical) limits of accuracy, which means that even small misalignments can have a significant impact. Another point aside the equipment is the mask assignment in the post-processing of the spot image. The usage of a distinct threshold during mask generation introduces a small uncertainty.

A limitation for the maximum layer thickness (i.e., edge height) for the proposed SSU approach is the depth of field of the used objective lens. For the applicability of the method, all material stacks contained in the measurement spot must be in focus at the same time. This is ensured if the maximum step height contained in the measurement spot is smaller than half the depth of field. The depth of field depends on the NA and the wavelength.[28] Measurements show that the depth of field for the used objective lens (100x, NA 0.75) is  $\approx 1 \mu m$  (for a detailed analysis of the depth of field for the employed setup see Figure \$5, Supporting Information). 1 µm should be a good estimation for lenses with 100x magnification for visible light, even for apochromatic objective lenses with a NA up to 0.95. This value is no obstacle for the application area of van der Waals materials, as the flake thicknesses used in devices are typically well below 1 um and usually even below 100 nm.[8,30,31] In addition, it can be assumed that with increasing edge height, the aforementioned contribution from the transition area increases. This must be considered for the maximum layer thickness, whereby this work demonstrates that a step height of up to 100 nm is possible.

## 3. Conclusion

By combining microspectroscopic reflectance measurements with the imaging capability inherent in such measurement systems, we demonstrate a significant improvement in the ability to obtain spectral information from samples with dimensions smaller than the measurement spot. For the exemplarily investigated samples, the determined thickness exhibits a maximum error of less than 10%, even in the limit when the examined material stacks only cover up to 20% of the area of the measurement spot. Simulations based on wave optics considering the complex diffraction phenomena at the edge region corroborate that the assumption of linear superposition of the different reflectance components of the material stacks located in the measurement spot, while neglecting the deviating reflectance around the edge within the TMM based modeling, is justified.

The simple combination of magnifying optics, spectroscopy, and imaging via our SSU method enables cost-effective, reliable, and non-destructive characterization of samples with lateral dimensions even well below 5 micrometers. In particular, mechanically exfoliated flakes of van der Waals materials are

www.advancedsciencenews.com



www.advopticalmat.de

used in a wide range of scientific applications. Our method can also be useful for heterostructures of van der Waals materials. Such heterostructures are widely used in photonics, [32–34] optics, [1] optoelectronics, [4,35] and medical technology. [36] Homogeneous surfaces of these materials that are not covered by metal contacts or other materials are often minuscule in according devices and can be precisely investigated employing our SSU approach. Furthermore, the method can also be used to reduce the resolvable structure size of the rather large measurement spot of objective lenses with low magnification and thus emulate the diameter of measurement spots of objective lenses with high magnification. Likewise, the reflectance of material stacks within periodic structures, as often found in nano- and microelectronics, can be assessed, although the structures clearly protrude beyond the measurement spot.

## 4. Experimental Section

Specimen Preparation: HOPG flakes were mechanically exfoliated on in-house grown 300 nm  $\mathrm{SiO}_2/\mathrm{Si}$  substrates under atmospheric conditions. Additionally, a 100 nm  $\mathrm{SiO}_2$  film was thermally grown on Si, and subsequently structured using a photo resist and optical lithography, followed by wet chemical etching. Finally, the  $\mathrm{SiO}_2$  thickness was determined by laser ellipsometry (LE). For the HOPG samples, the reference thickness was determined using a Bruker Dimension ICON AFM system in intermittent-contact mode.

Reflectance Measurement: All reflectance measurements were performed with an Axio Imager Z2 system by Zeiss equipped with a 100x/NA 0.75 objective lens and an attached spectrometer, as depicted in Figure 1a. The light source was a halogen lamp and therefore the spectral range was limited from 440–950 nm. The diameter of the circular measurement spot was ca. 18 µm, determined by the magnification of the system and the diameter of the glass fiber. In addition, there was a variable spot diaphragm in the detection path, enabling the seamless adjustment of the measured area to rectangular or squared shapes with smaller dimensions. Within the SSU method, the use of more common circular iris diaphragms is also possible. For homogeneous specimens, the measured reflectance was independent from the configuration of the spot diaphragm (see Figure S6, Supporting Information for a comparison of the reflectance for different settings). For small samples, the spot diaphragm was used to limit the measurement spot. Nevertheless, care had to be taken that the diaphragm was not set too small since otherwise diffracted light could couple into the objective lens (see Figure S7, Supporting Information for an exemplary analysis of the impact of stray light in the reach of edges). A silicon sample was used as reference to obtain absolute reflectance values, since the reflectance spectrum for Si is well-known in the respective wavelength range. All spectra were averaged over 10 acquisitions. For the SiO<sub>2</sub> sample the complete circular measurement spot with a diameter of 18 μm was used with the spot diaphragm open while for the small HOPG samples the spot diaphragm was set to 5  $\mu m \times 5 \mu m$ , demonstrating the general applicability of the SSU method regardless of the presence or shape of an additional spot diaphragm. For each sample, different values of area percentages were achieved by moving the microscope stage transversely to a material edge in small steps and an image was taken at each position (for an example see Figure 2b).

Data Processing and Modeling: An image of the shape of the measurement spot (depending on the spot diaphragm) was captured by illuminating the glass fiber from the spectrometer side. The image was converted to gray values and a mask of the measurement spot was created using bilateral filtering<sup>[37]</sup> and subsequent thresholding<sup>[38]</sup> (see Figure S8a,b, Supporting Information). The mask was then applied to the gray scale image of the specimen and the histogram of the area within the measurement spot was calculated, with the x-axis representing increasing gray values (cf. Figures S1b and S2b, Supporting Information). From the histogram, the gray levels with the most pixel counts were identified for the two materi-

als and the minima on the left and right of these peaks were considered as boundaries. The gray value between the right boundary of the dark material and the left boundary of the bright material was defined as transition area. All pixels to the left of the transition area were assigned to the dark material and all pixels to the right to the bright material (see Figure S8c, Supporting Information for an example of histogram evaluation). Then the area fractions of the two materials were determined by dividing the number of pixels in the histogram assigned to one material by the total number of pixels in the measurement spot. As a means of validating the determined area coverage, the integral of the reflectance contrast was calculated for the respective measurement series. This shows a good agreement with the expected area fractions (for a detailed analysis see Figure S9, Supporting Information).

For the modeling, the influence of the objective lens with a high NA has to be considered as described in the previous work. The objective lens dependent factor was specified as 2 and the thickness of the layer of interest was determined via least square fitting of the modeled and measured spectra. The refractive indices of air, silicon, silicon, so SSU in Figures 2c and 3 were acquired by assuming a single material stack filling the whole measurement spot. For the proposed SSU approach, the different material stacks in the measurement spot were taken into account with their respective area coverage within the modeled reflectance  $R_{Tot}$  in the measurement spot as follows:

$$R_{Tot} = c_{Bright} R_{Bright} + c_{Dark} R_{Dark} \tag{1}$$

where  $c_{Bright}$  and  $c_{Dark}$  are the calculated area fractions and  $R_{Bright}$  and  $R_{Dark}$  the corresponding reflectance spectra of the according material stacks. Depending on which of the material stacks was the one to be examined (i.e. the one for which no measured spectrum with the measurement spot fully covering that material stack is available), the relevant thickness was determined via least square fitting. For the contribution of the substrate in Equation (1) ( $R_{Bright}$  or  $R_{Dark}$  depending on the RGB values in comparison to the examined material stack) the measured reflectance for a completely homogeneous coverage of the measurement spot for the reflectance spectrum of the substrate is easily fulfilled in most cases of van der Waals materials due to the mesa-like morphology and nanometer-scale thickness. To avoid the influence of possible inaccuracies in the modeling of the reflectance of the substrate, the measured reflectance of the substrate was explicitly used for the modeling of  $R_{Tot}$ .

To illustrate this process using the example of the HOPG samples, HOPG appears brighter than the substrate in both cases on a micrograph. The HOPG is therefore used as  $R_{Bright}$  in Equation (1) and the substrate as  $R_{Dark}$ . A reflectance measurement with 100% coverage of the measurement spot is easily possible for the homogeneous substrate and this measurement is used for  $R_{Dark}$  in Equation (1).  $R_{Tot}$  is then modeled using the area fractions determined from the histogram and compared with the measurement, whereby the thickness of the HOPG is varied in the model and the optimum value is determined via least square fitting, as described in Ref. [7].

### Supporting Information

Supporting Information is available from the Wiley Online Library or from the author.

## Acknowledgements

Financial support by the German Research Foundation (DFG) via the project 454726051 "Electronic devices based on the 2D material black phosphorus – layer-dependent properties," (grant no. HU 2827/2-1 and KR 2264/7-1) is gratefully acknowledged. N.V. acknowledges funding by the Deutsche Forschungsgemeinschaft (DFG, German Research Foundation)— Project-ID 416229255 – SFB 1411.

Open access funding enabled and organized by Projekt DEAL.

2195 1071, 2025, 5, Down

inced.onlinelibrary.wiley.com/doi/10.1002/adom.202402502 by Forschungszentrum

Jülich GmbH Research Center, Wiley Online Library on [21/02/2025]. See the Terms

on Wiley Online Library for rules of use; OA articles are governed by the applicable Creative Commons License



#### **Conflict of Interest**

The authors declare no conflict of interest.

## **Author Contributions**

J.S. and M.N. contributed equally to this work. J.S., M.N., and L.R. conducted the spectroscopic measurements. The study was instituted by A.H., M.R., M.K-G., and V.K. Samples were prepared by M.N. Analysis and data selection were carried out by J.S. and M.N. The code for the image evaluation was implemented by J.S. based on the concept of A.P. The SSU model was implemented by M.R. and J.S. The code for the wave optic simulations was created by P.E. Discussions on modeling were performed with participation of M.N. and A.H. The draft was written by J.S. and M.N. with annotations by A.H., M.R., M.K.-G.,V.K., and N.V. A.H., N.V., and V.K. supervised the project. All authors commented on the manuscript.

# **Data Availability Statement**

The data that support the findings of this study are openly available in Zenodo at https://doi.org/10.5281/zenodo.13753754, reference number 13753754.

## **Keywords**

2D materials, graphite, reflectance, thin films, transfer matrix method

Received: September 15, 2024 Revised: November 28, 2024 Published online: December 29, 2024

- [1] S. A. Dereshgi, Y.-S. Lee, M. C. Larciprete, M. Centini, V. P. Dravid, K. Aydin, Adv. Opt. Mater. 2023, 11, 2202603.
- [2] C. Trovatello, A. Marini, M. Cotrufo, A. Alù, P. J. Schuck, G. Cerullo, ACS Photonics 2024, 11, 2860.
- [3] W. Wu, Z. Liu, Z. Qiu, Z. Wu, Z. Li, X. Yang, L. Han, C. Li, N. Huo, X. Wang, J. Yao, Z. Zheng, J. Li, Adv. Opt. Mater. 2024, 12, 2301410.
- [4] R. Zhang, B. Duan, R. Wang, Y. Fan, J. Chu, Adv. Opt. Mater. 2023, 11, 2201828.
- [5] C. Hsu, R. Frisenda, R. Schmidt, A. Arora, S. M. de Vasconcellos, R. Bratschitsch, H. S. J. v. d. Zant, A. Castellanos-Gomez, Adv. Opt. Mater. 2019, 7, 1900239.
- [6] A. Hutzler, B. Fritsch, C. D. Matthus, M. P. M. Jank, M. Rommel, Sci. Rep. 2020, 10, 13676.
- [7] J. Schwarz, M. Niebauer, M. Koleśnik-Gray, M. Szabo, L. Baier, P. Chava, A. Erbe, V. Krstić, M. Rommel, A. Hutzler, Small Methods 2023, 7, 2300618.
- [8] C. D. Matthus, P. Chava, K. Watanabe, T. Taniguchi, T. Mikolajick, M. Helm, A. Erbe, *IEEE J. Electron Devices Soc.* 2023, 11, 359.
- [9] M. Koleśnik-Gray, L. Meingast, M. Siebert, T. Unbehaun, T. Huf, G. Ellrott, G. Abellán, S. Wild, V. Lloret, U. Mundloch, J. Schwarz, M. Niebauer, M. Szabo, M. Rommel, A. Hutzler, F. Hauke, A. Hirsch, V. Krstić, npj 2D Mater. Appl. 2023, 7, 21.
- [10] R. H. Muller, J. C. Farmer, Surf. Sci. 1983, 135, 521.
- [11] O. Luria, P. K. Mohapatra, A. Patsha, A. Kribus, A. Ismach, Appl. Surf. Sci. 2020, 524, 146418.
- [12] G. Isic, M. Jakovljevic, M. Filipovic, D. M. Jovanovic, B. Vasic, S. Lazovic, N. Puac, Z. L. Petrovic, R. Kostic, R. Gajic, J. Humlicek, M. Losurdo, G. Bruno, I. Bergmair, K. Hingerl, J. Nanophotonics 2011, 5, 051809.

- [13] G. Cardenas-Chirivi, C. Navarrete, D. Lozano, C. A. Herre no-Fierro, Y. Hernandez, Opt. Mater. 2022, 133, 112890.
- [14] E. Houser, T. V. Mc Knight, J. M. Redwing, F. C. Peiris, J. Cryst. Growth 2024, 640, 127741.
- [15] N. Blayo, R. A. Cirelli, F. P. Klemens, J. T. C. Lee, J. Opt. Soc. Am. A 1995, 12, 591.
- [16] S.-J. Cho, P. G. Snyder, N. J. Ianno, C. M. Herzinger, B. Johs, *Thin Solid Films* 2004, 455-456, 645.
- [17] P. A. Heimann, R. J. Schutz, J. Electrochem. Soc. 1984, 131, 881.
- [18] S. Bosch-Charpenay, J. Xu, J. Haigis, P. A. Rosenthal, P. R. Solomon, J. M. Bustillo, J. Microelectromech. Syst. 2002, 11, 111.
- [19] E. J. Klein, W. F. Ramirez, J. L. Hall, Rev. Sci. Instrum. 2001, 72, 2455.
- [20] J. Bauer, O. Fursenko, S. Marschmeyer, F. Heinrich, F. Villasmunta, C. Villringer, C. Zesch, S. Schrader, J. Vac. Sci. Technol., B 2019, 37, 062205.
- [21] Y.-S. Ku, J. Micro/Nanolithography, MEMS, MOEMS 2014, 13, 011209.
- [22] B. Zou, Y. Zhou, Y. Zhou, Y. Wu, Y. He, X. Wang, J. Yang, L. Zhang, Y. Chen, S. Zhou, H. Guo, H. Sun, Nano Res. 2022, 15, 8470.
- [23] R. Rani, A. Kundu, K. S. Hazra, Opt. Mater. 2019, 90, 46.
- [24] Y. Niu, S. Gonzalez-Abad, R. Frisenda, P. Marauhn, M. Drüppel, P. Gant, R. Schmidt, N. S. Taghavi, D. Barcons, A. J. Molina-Mendoza, S. M. de Vasconcellos, R. Bratschitsch, D. Perez De Lara, M. Rohlfing, A. Castellanos-Gomez, *Nanomaterials* 2018, 8, 9.
- [25] A. Hutzler, C. D. Matthus, M. Rommel, L. Frey, Appl. Phys. Lett. 2017, 110, 021909.
- [26] A. Hutzler, C. D. Matthus, C. Dolle, M. Rommel, M. P. M. Jank, E. Spiecker, L. Frey, J. Phys. Chem. C 2019, 123, 9192.
- [27] T. Fühner, T. Schnattinger, G. Ardelean, A. Erdmann, Optical Microlithography XX, SPIE Proceedings, (Ed: D. G. Flagello), SPIE, Washington 2007, p. 65203F.
- [28] Handbook of Optics, 2nd ed., (Ed: M. Bass) vol. 2, McGraw-Hill, New York 1995
- [29] X. Pan, N. Rahimi, A. Price, A. Ghasempour, F. C. Ndi, in *Proc. SPIE* 10925, Photonic Instrumentation Engineering VI, (Ed.: Y. G. Soskind), SPIE, Washington 2019, p. 109250S.
- [30] Y. Fan, Q. Wan, Q. Yao, X. Chen, Y. Guan, H. Alnatah, D. Vaz, J. Beaumariage, K. Watanabe, T. Taniguchi, J. Wu, Z. Sun, D. Snoke, ACS Photonics 2024, 11, 2722.
- [31] H. J. Jin, C. Park, H. H. Byun, S. H. Park, S.-Y. Choi, ACS Photonics 2023, 10, 3027.
- [32] S. Moon, J. Kim, J. Park, S. Im, J. Kim, I. Hwang, J. K. Kim, Adv. Mater. 2023, 35, 2204161.
- [33] L. Zhang, H. Hu, Y. Zhou, J. Miao, G. Ouyang, X. Chen, ACS Photonics 2022.
- [34] W. Wen, L. Wu, T. Yu, ACS Mater. Lett. 2020, 2, 1328.
- [35] A. Kumar, L. Viscardi, E. Faella, F. Giubileo, K. Intonti, A. Pelella, S. Sleziona, O. Kharsah, M. Schleberger, A. Di Bartolomeo, J. Mater. Sci. 2023, 58, 2689.
- [36] H. Zhang, T. Fan, W. Chen, Y. Li, B. Wang, Bioactive Mater. 2020, 5, 1071
- [37] C. Tomasi, R. Manduchi, in Sixth Int. Conf. on Computer Vision (IEEE Cat. No.98CH36271), IEEE, New York 1998, pp. 839–846.
- [38] N. Otsu, IEEE Trans. Syst., Man, Cybern. 1979, 9, 62.
- [39] E. R. Peck, K. Reeder, J. Opt. Soc. Am. A 1972, 62, 958.
- [40] M. A. Green, Sol. Energy Mater. Sol. Cells 2008, 92, 1305.
- [41] A. Boosalis, Ph.d. dissertation, University of Nebraska-Lincoln, Lincoln 2015.
- [42] G. Bradski, Dr. Dobb's J. Software Tools 2000.
- [43] M. Born, E. Wolf, P. Knight, *Principles of Optics*, 7-th anniversary edition, 60th anniversary of first edition, 20th anniversary of seventh edition edition, Cambridge University Press, Cambridge, 2019.